Nrf2 Is Commonly Activated in Papillary Thyroid Carcinoma, and It Controls Antioxidant Transcriptional Responses and Viability of Cancer Cells

Panos G. Ziros,* Stavroula D. Manolakou,* Ioannis G. Habeos, Ioannis Lilis, Dionysios V. Chartoumpekis, Vasiliki Koika, Paula Soares, Venetsana E. Kyriazopoulou, Chrisoula D. Scopa, Dionysios J. Papachristou, and Gerasimos P. Sykiotis

Department of Internal Medicine (P.G.Z., S.D.M., I.G.H., D.V.C., V.K., V.E.K., G.P.S.), Division of Endocrinology, University of Patras Medical School, 26500 Patras, Greece; Interdepartmental Postgraduate Program in Medicinal Chemistry (S.D.M.), Drug Discovery and Design, University of Patras, 26500 Patras, Greece; Department of Anatomy, Histology, and Embryology (I.L., D.J.P.), University of Patras Medical School, 26500 Patras, Greece; Institute of Molecular Pathology and Immunology of the University of Porto (P.S.), Cancer Biology Group, 4200-465 Porto, Portugal; Department of Pathology (C.D.S.), University of Patras Medical School, 26500 Patras, Greece; and Department of Pathology (D.J.P.), University of Pittsburgh, School of Medicine, Pittsburgh, Pennsylvania 15261

Context: The antioxidant transcription factor NFE2-related factor 2 (Nrf2), encoded by *NFE2L2*, has been implicated as mediator of thyroid cancer cell line resistance to proteasome inhibitors. However, the activity status of the Nrf2 pathway in human thyroid cancer remains unknown.

Objective: The aims of this study were assessment of the activity status of the Nrf2 pathway in papillary thyroid carcinoma (PTC) and investigation of its role(s) in antioxidant transcriptional responses and viability of cancer cells.

Design and Setting: We conducted retrospective immunohistochemical analyses of PTC specimens, adjacent normal tissue, and benign lesions; assays of viability and gene expression in the PTC cell lines K1 and TPC-1 after genetic/pharmacological manipulation of Nrf2; and DNA sequencing at an academic medical center.

Patients: The study included 42 PTC and 42 benign lesions (24 adenomas and 18 nodular hyperplasias).

Main Outcome Measures: We assessed the abundance of Nrf2, Nqo1, Keap1, and 4HNE; cell line viability and mRNA expression of *Nrf2*, *Nqo1*, and *Trdx1*; and the sequence of *NFE2L2*, *KEAP1*, and *BRAF*.

Results: Nrf2 and its target Nqo1 were undetectable in normal tissue; their levels were significantly higher in PTC than in benign lesions ($P < .0001$ and $P = .024$, respectively). The Nrf2 inhibitor Keap1 was variably abundant in PTC, and its levels did not correlate with Nrf2 ($P = .37$), arguing against decreased levels as the mechanism for Nrf2 activation. The oxidized lipid 4HNE was more abundant in PTC than normal tissue ($P < .001$), indicating oxidative stress. Nrf2 mediated transcriptional antioxidant responses in both the PTC cell lines K1 and TPC-1 and in the nontransformed cell line TAD2, but it conferred a viability advantage specifically in the PTC cell lines.

Conclusions: The high activity of Nrf2 in PTC warrants further exploration of this pathway's potential diagnostic, prognostic, and/or therapeutic utility in PTC. **(*J Clin Endocrinol Metab* 98: E1422–E1427, 2013)**

ISSN Print 0021-972X ISSN Online 1945-7197
Printed in U.S.A.

Received February 27, 2013. Accepted June 7, 2013.
First Published Online June 13, 2013

* P.G.Z. and S.D.M. contributed equally and are co-first authors.

Abbreviations: FBS, fetal bovine serum; Keap1, Kelch-like ECH-associated protein 1; Nrf2, NFE2-related factor 2; PTC, papillary thyroid carcinoma; siRNA, small interfering RNA.

The thyroid has a high capacity for defense against oxidative stress (1), likely because a minimal oxidative load is a prerequisite for its normal function (2, 3). Specific antioxidant/detoxification enzymes such as peroxiredoxin 5 and thioredoxin reductase 1 presumably enable thyrocytes to maintain homeostasis by ameliorating oxidative insults (3, 4), yet the mechanisms controlling their expression remain insufficiently elucidated.

Nrf2 (NFE2-related factor 2), encoded by *NFE2L2* (NFE2-like 2), mediates a transcriptional response to oxidative stress in various tissues (5). In basal conditions, Nrf2 is targeted for proteasomal degradation by its cytoplasmic inhibitor, Kelch-like ECH-associated protein 1 (Keap1). When oxidants react with redox-sensitive cysteines of Keap1, Nrf2 degradation is abolished and Nrf2 accumulates in the nucleus where it transactivates protective genes such as *Nqo1* [NAD(P)H dehydrogenase quinone 1]. By preventing oxidation of macromolecules, Nrf2 protects organisms across the evolutionary spectrum against stress-related pathologies (6).

However, as a protective system, Nrf2 signaling can also confer benefits on cancer cells: constitutive Nrf2 activation by somatic mutations or epigenetic events is found in various human cancers and promotes chemoresistance (7–10). Conversely, chemosensitivity is increased in cancers with low Nrf2 activity due to overactive degradation systems (11). Recently, studies in thyroid cancer cell lines implicated Nrf2 as mediator of resistance to the chemotherapeutic activity of proteasome inhibitors, and thus as a potential new target in thyroid cancer (12, 13). However, the clinical relevance of these findings is uncertain because the activity of Nrf2 in human thyroid cancer remains unknown. In this study, we aimed to assess the activity of the Nrf2 pathway in papillary thyroid carcinoma (PTC) and to investigate its role(s) in the antioxidant responses and viability of cancer cells.

Materials and Methods

Specimens

We analyzed 42 archived formalin-fixed, paraffin-embedded surgical specimens from PTC and 42 from benign lesions (24 adenomas, 18 nodular hyperplasias). Specimens were reviewed by experienced pathologists (D.J.P. and C.D.S.) to confirm the diagnosis according to standard criteria (14) and to identify cancer, benign lesion, and normal tissue areas. The study was approved by the University of Patras Institutional Review Board.

Immunohistochemistry

After deparaffinization in xylene and rehydration in graded ethanols, standard immunohistochemistry was performed as previously described (15). Primary antibodies used were: anti-Nrf2 (sc-13032 and sc-722, dilution 1:100; Santa Cruz Biotechnology, Santa Cruz, California; and HPA002990, dilution 1:100; Atlas Antibodies AB, Stockholm, Sweden); anti-Nqo1 (sc-32793, dilution 1:70, Santa Cruz Biotechnology); anti-Keap1 (ab119403, dilution 1:100; Abcam Inc., Cambridge, Massachusetts); and anti-4HNE (ab46545, dilution 1:350, Abcam Inc.). Specific binding was detected with the Envision kit (Dako, Glostrup, Denmark), and the color reaction was visualized with 3,3′-diaminobenzidine. For negative controls, blocking solution was added instead of primary antibody. In pilot experiments, the 3 independent anti-Nrf2 antibodies yielded matching patterns, indicating specificity of the staining (Supplemental Figure 1, published on The Endocrine Society's Journals Online web site at http://jcem.endojournals.org); sc-13032 was selected for further use.

Because in the immunopositive cases of PTC the examined molecules were detected in virtually all evaluated cells, we did not assess the percentage of positive cells but assessed the staining intensity, which was scored on a scale of 0 to 3(+): 0, no immunoreactivity; 1(+), weak; 2(+), moderate; 3(+), strong.

Cell culture

The PTC cell line K1 (from the European Collection of Cell Cultures) carrying a *BRAF* V600E mutation (16) was maintained in RPMI. The PTC cell line TPC-1 (from Prof. Marc Mareel) harboring a *RET/PTC* rearrangement (17) was maintained in DMEM. The immortalized fetal thyroid cell line TAD2 (18) (from Drs Terry Davies and Rauf Latif) was maintained in RPMI. Cells were cultured at 37°C, 5% CO_2 in a humidified incubator in specified medium with 10% fetal bovine serum (FBS) and 1% streptomycin/penicillin. Culture media and supplements were from Invitrogen. For Western immunoblotting and analysis of protein oxidation, see Supplemental Data.

RNA interference and compound treatments

Nrf2 knockdown was performed using stealth small interfering RNA (siRNA) from Invitrogen (HSS107130); a negative siRNA (12935-200; Invitrogen) was used as control. Cells were transfected at a final siRNA concentration of 40 nmol/L by the reverse transfection method using Lipofectamine RNAiMax (Invitrogen) according to the manufacturer's protocol. For gene expression assays, cells were transfected in 12-well plates in complete medium for 24 hours, and then treated with 5 μM sulforaphane (Sigma, St Louis, Missouri) or 0.1% dimethyl sulfoxide for another 24 hours in medium containing 0.5% FBS. For cell viability assays, cells were transfected in 96-well plates in complete medium, and after 24 hours they were incubated for 48 hours with medium containing 0.5% FBS and supplemented with 1 or 5 μM vemurafenib (PLX4032; Selleck Chemicals, Houston, Texas) or 0.1% dimethyl sulfoxide.

Real-time RT-PCR

Total cell RNA was isolated using TRIzol (Invitrogen) and further purified using the RNeasy mini-kit with DNAse digestion (QIAGEN, Valencia, California). cDNA was synthesized using the Superscript first-strand synthesis system (Invitrogen), and real-time PCRs were performed on a StepOnePlus instrument (Applied Biosystems, Foster City, California) using FAST SYBR green (Kapa Biosystems, Woburn, Massachusetts): 3 minutes at 95°C, followed by 40 cycles of 10 seconds at 95°C and 30 seconds at 60°C. Relative gene expression was calculated by the

comparative cycle threshold method using *GAPDH* and *TBP* as reference genes. Primers are shown in Supplemental Table 1.

Cell viability assay

The CellTiter-Glo Luminescent Cell Viability Assay Kit (Promega, Madison, Wisconsin) determines the number of viable cells in culture based on quantification of ATP, which reflects the presence of metabolically active cells. Briefly, 72 hours after transfection, K1 or TPC-1 cells treated as above were lysed by adding 100 μL CellTiter-Glo reagent to each well containing 100 μL cell culture medium. The luminescence intensity was measured 10 minutes later on a Victor3 plate reader (Perkin-Elmer, Wellesley, Massachusetts).

DNA sequencing

Genomic DNA was extracted from dissected cancer specimens using the Nucleospin FFPE DNA kit (Macherey-Nagel, Düren, Germany), and from K1 and TPC-1 cells using standard phenol-chloroform procedure. Primers and PCR conditions for the coding exons of *KEAP1* and exon 2 of *NFE2L2* were as published (7, 8). DNA was amplified by PCR with Platinum Taq DNA Polymerase (Invitrogen) supplemented with a homemade PCR enhancer under conditions previously described (19). Both strands were sequenced utilizing the PCR primers. For *BRAF* exon 15, primers 5′-TCATAATGCTTGCTCTGATAGGA-3′ and 5′-GGCCAAAAATTTAATCAGTGGA-3′ were used for PCR and sequencing. PCR conditions were: 4 minutes at 95°C; 35 cycles of 30 seconds at 95°C, 30 seconds at 51°C, and 45 seconds at 72°C; and 10 minutes at 72°C.

Statistics

For immunohistochemistry data, the Mann-Whitney test was used for differences between independent samples; the Spearman rank-order correlation coefficient was used for correlations of matched data; and the Wilcoxon signed-rank test was used for differences between matched samples. Tests (always 2-tailed) were performed using IBM SPSS Statistics (IBM Corporation, Armonk, New York).

For cell culture studies, ≥3 different experiments were performed on different days. Student's *t* test or 1-way ANOVA with Tukey post test was performed using Prism 5 (GraphPad Software, Inc, San Diego, California).

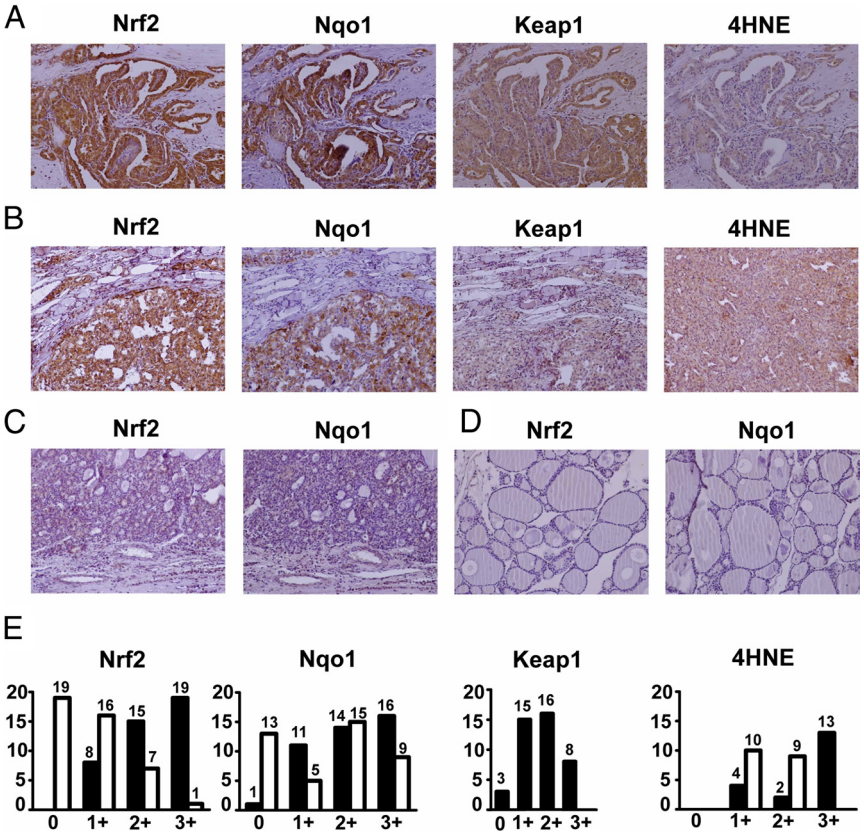

Figure 1. Immunohistochemical detection of Nrf2, Nqo1, Keap1, and 4HNE in PTC and benign thyroid lesions. A, Representative PTC specimen. Scores were: Nrf2, 3(+); Nqo1, 3(+); Keap1, 2(+); 4HNE, 1(+). As expected, Nrf2 stain was seen both in the cytoplasm and in nuclei; Nqo1 and Keap1 were detected in the cytoplasm; and 4HNE was detected primarily in the cytoplasm. Original magnification, ×20. B, Representative follicular variant of PTC specimen. Scores were: Nrf2, 3(+); Nqo1, 3(+); Keap1, 1(+); 4HNE, 2(+). C, Representative adenoma specimen. Scores were: Nrf2, 1(+); Nqo1, 0. D, Representative nodular hyperplasia specimen. Scores were: Nrf2, 0; Nqo1, 0. E, Summary of the scores in benign lesions (white bars) and PTC (black bars). Y-axis, number of specimens; X-axis, staining score.

Results

The Nrf2 pathway is commonly activated in PTC

In normal thyroid tissue, Nrf2 and its target Nqo1 were undetectable in follicular cells under the conditions employed. In most PTC specimens Nrf2 staining of tumor cells was strong or moderate (few showed weak staining and none were negative) (Figure 1 and Supplemental Table 2), whereas it was weak or negative in most benign lesions ($P < .0001$). Similarly, Nqo1 staining was stronger in PTC than in benign lesions ($P = .024$) (Figure 1 and Supplemental Table 2). These data indicate that the Nrf2 pathway is commonly activated in PTC, whereas it is only occasionally activated in benign thyroid lesions.

There was no significant correlation of Nrf2 or Nqo1 abundance with the various histological subtypes of PTC, such as the follicular variant ($P = .91$ and $P = .84$, respectively), or subtypes associated with a varied or more aggressive behavior (tall cell, solid/trabecular, diffuse sclerosing, and/or oxyphilic variant; $P = .80$ and $P = .50$, respectively); with lymph metastasis ("N", $P = .17$

and $P = .83$, respectively); or with age ($P = .40$ and $P = .66$, respectively) at the time of thyroidectomy (Supplemental Table 2). Notably, the abundance of Nqo1 (but not of Nrf2) correlated significantly with tumor size/local invasion ("T", $P = .02$ and $P = .19$, respectively); higher T correlated with relatively lower Nqo1 abundance. In addition, whereas there was a significant positive correlation between Nrf2 and Nqo1 abundance in benign lesions ($P = .02$), there was no correlation in PTC ($P = .49$).

Further studies inquired into the potential mechanism(s) of Nrf2 activation in PTC. A random subset of specimens (n = 11) expressing Nrf2 strongly (n = 8) or moderately (n = 3) were sequenced for the *BRAF* V600E mutation, which was present (heterozygous) in 6 of 11 (Supplemental Table 2), suggesting that Nrf2 activation is not always associated with BRAF mutational activation. These specimens were also negative for mutations in *KEAP1* or in *NFE2L2* exon 2, encoding the Keap1-interacting domain. Keap1 showed variable abundance in PTC (Figure 1 and Supplemental Table 2), and its levels did not correlate with Nrf2 levels ($P = .37$), arguing against decreased Keap1 levels as a ubiquitous mechanism for Nrf2 activation. The oxidized lipid 4HNE was strongly present in most specimens; among the 19 samples with available matched normal tissue, 4HNE levels were higher in the carcinomas (Figure 1 and Supplemental Table 2) ($P < .001$).

Nrf2 signaling regulates antioxidant responses and viability of PTC cell lines

The PTC cell lines K1 and TPC-1 and the noncancerous human thyroid cell line TAD2 were used to assay gene expression and viability in response to pharmacological or genetic manipulation of Nrf2. Genomic DNA sequencing showed no mutations in *KEAP1* or in *NFE2L2* exon 2, encoding the Keap1-interacting domain. Patterns of mRNA expression and protein abundance of Nrf2 pathway components in the cell lines (Supplemental Figures 2 and 3) paralleled the immunohistochemistry patterns seen in PTC specimens (Figure 1), supporting the validity of these cellular models. Oxidative damage at basal conditions was highest in the TAD2 cells, intermediate in the K1 cells, and lowest in the TPC-1 cells (Supplemental Figure 3). In all cell lines, treatment with the Nrf2 activator sulforaphane significantly increased the mRNA of the prototypical Nrf2 target gene *Nqo1* and of the antioxidant enzyme *Txnrd1* (Figure 2, A–C). Nrf2 knockdown significantly repressed the basal expression of *Nqo1* and, in K1 cells, of *Txnrd1*, and abolished the sulforaphane-mediated induction of both genes (Figure 2, A–C). These data demonstrate that Nrf2 regulates antioxidant transcriptional responses in PTC and normal thyroid cells. Nrf2 knockdown also significantly decreased viability of the PTC cell lines, mimicking the effect of the BRAF inhibitor vemurafenib (Figure 2, D and E). Viability of TAD2 cells was not af-

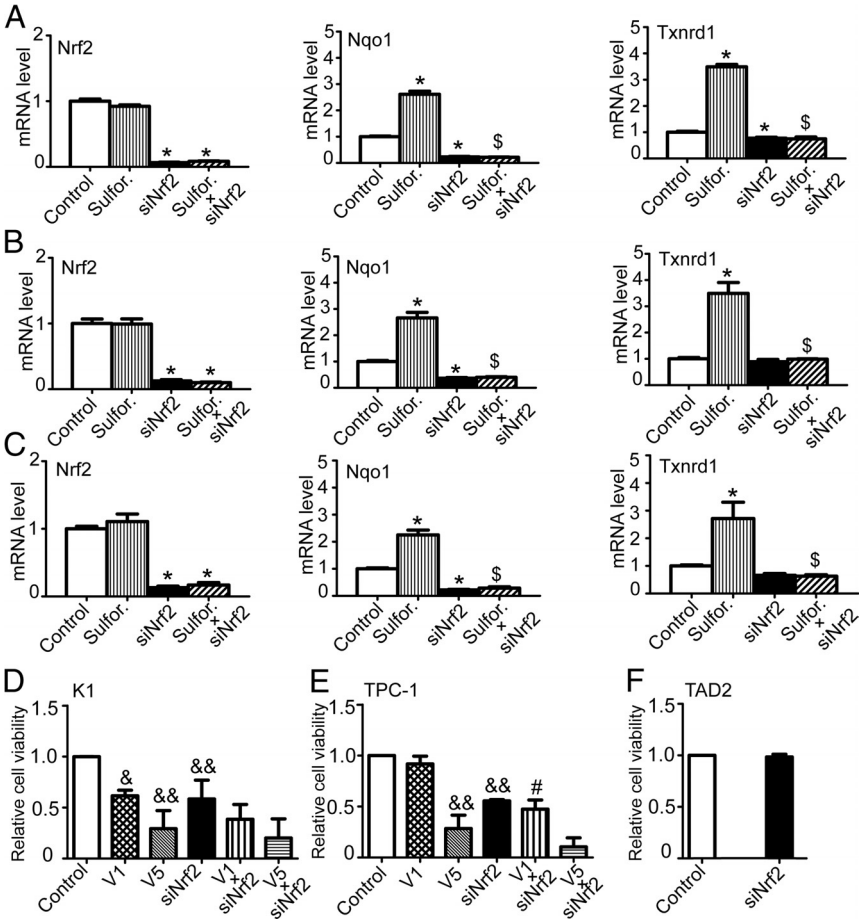

Figure 2. mRNA quantification and viability of K1, TPC-1, and TAD2 cells in response to pharmacological or genetic manipulation of Nrf2. A, mRNA levels in K1 cells in which Nrf2 is activated by treatment with sulforaphane or knocked down by RNA interference. B, mRNA levels in TPC-1 cells treated as in panel A. C, mRNA levels in TAD2 cells treated as in panels A and B. D, Viability assay on K1 cells treated with the tyrosine kinase inhibitor vemurafenib or with siRNA targeting Nrf2. E, Viability assay on TPC-1 cells treated as in panel D. F, Viability assay on TAD2 cells treated with siRNA targeting Nrf2. Bars, means ± SD; sulfor., 5 μM sulforaphane; V1, 1 μM vemurafenib; V5, 5 μM vemurafenib; *, $P < .001$ compared to control; $, $P < .001$ compared to sulforaphane; &, $P < .01$ compared to control; &&, $P < .001$ compared to control; #, $P < .01$ compared to V1.

fected by siRNA targeting Nrf2 (Figure 2F), indicating a specific role for Nrf2 in the viability of PTC cells.

Discussion

Although interest in oxidative stress and the thyroid is mounting, very little is known about Nrf2 in the thyroid. Two recent studies in thyroid cancer cell lines (mostly anaplastic) showed that Nrf2 mediates resistance to proteasome inhibitors (12, 13) and emphasized the need to establish the clinical relevance of Nrf2 by characterizing its activity in human thyroid cancer. By demonstrating that the Nrf2 pathway is commonly activated in PTC and that it regulates antioxidant responses and viability of cancer cells, the present study highlights Nrf2 as a new hallmark of PTC. Its potential utility in distinguishing PTC from benign nodules in fine-needle aspiration material and/or in treating advanced or refractory PTC warrants further exploration.

The lack of *KEAP1* and *NFE2L2* mutations among specimens with high Nrf2 abundance suggests that activation of the pathway in PTC is secondary to some other phenomenon. Nrf2 activation in other cancer types has been linked to increased *NFE2L2* transcription due to *BRAF* or *KRAS* mutations (10); whereas the *BRAF* V600E mutation was found in 6 of 11 specimens, *KRAS* was not analyzed due to the special technical requirements involved (20). Reduced *KEAP1* expression from increased promoter methylation has also been reported as an activating mechanism (9), but Keap1 abundance was variable among PTC specimens. The increased oxidative stress evident in PTC herein and in previous work (21) may contribute to Nrf2 activation; alternatively, or additionally, it may indicate that Nrf2 activation is insufficient to fully restore redox balance in PTC, as suggested also by the ability to further activate the pathway in the K1 and TPC-1 cell lines. Although in the biopsy specimens, higher levels of oxidative damage were observed in PTC samples compared to benign tumors, among the (rapidly growing) cell lines, the highest levels of oxidative damage were observed in the noncancerous TAD2 cells. Thus, the exact cause-and-effect relationship between oxidative damage and Nrf2 activity in PTC remains to be elucidated. Furthermore, the lack of correlation between Nrf2 and Nqo1 abundance in PTC and the inverse correlation of Nqo1 abundance with the carcinoma T suggest that regulation and/or efficiency of the Nrf2 pathway in PTC are also perturbed.

Limitations of the present study due to its retrospective design and reliance on archived material include the lack of Nrf2 and target gene measurements at the mRNA level in the PTC specimens and the lack of prospective assessment of the prognostic value of Nrf2 activity status. Our ongoing studies will address these issues and also investigate Nrf2 signaling in follicular differentiated and anaplastic thyroid carcinomas, as well as in thyroid physiology and its various perturbations besides cancer.

Acknowledgments

Address all correspondence and requests for reprints to: Gerasimos P. Sykiotis, Department of Internal Medicine, Division of Endocrinology, University of Patras Medical School, 26500 Patras, Greece. E-mail: gsykiotis@upatras.gr.

This work was supported by Marie Curie International Reintegration Grant 268266/"thyroidantioxidant" (to G.P.S.). The source of funding is the European Commission Research Executive Agency.

Disclosure Summary: The authors have nothing to disclose.

References

1. **Maier J, van Steeg H, van Oostrom C, Paschke R, Weiss RE, Krohn K.** Iodine deficiency activates antioxidant genes and causes DNA damage in the thyroid gland of rats and mice. *Biochim Biophys Acta*. 2007;1773:990–999.
2. **Poncin S, Colin IM, Gerard AC.** Minimal oxidative load: a prerequisite for thyroid cell function. *J Endocrinol*. 2009;201:161–167.
3. **Poncin S, Van Eeckoudt S, Humblet K, Colin IM, Gerard AC.** Oxidative stress: a required condition for thyroid cell proliferation. *Am J Pathol*. 2010;176:1355–1363.
4. **Leoni SG, Kimura ET, Santisteban P, De la Vieja A.** Regulation of thyroid oxidative state by thioredoxin reductase has a crucial role in thyroid responses to iodide excess. *Mol Endocrinol*. 2011;25:1924–1935.
5. **Lee JM, Li J, Johnson DA, et al.** Nrf2, a multi-organ protector? *FASEB J*. 2005;19:1061–1066.
6. **Sykiotis GP, Bohmann D.** 2010 Stress-activated cap'n'collar transcription factors in aging and human disease. *Sci Signal*. 2010;3:re3.
7. **Singh A, Misra V, Thimmulappa RK, et al.** Dysfunctional KEAP1-NRF2 interaction in non-small-cell lung cancer. *PLoS Med*. 2006;3:e420.
8. **Shibata T, Ohta T, Tong KI, et al.** Cancer related mutations in NRF2 impair its recognition by Keap1-Cul3 E3 ligase and promote malignancy. *Proc Natl Acad Sci USA*. 2008;105:13568–13573.
9. **Wang R, An J, Ji F, Jiao H, Sun H, Zhou D.** Hypermethylation of the Keap1 gene in human lung cancer cell lines and lung cancer tissues. *Biochem Biophys Res Commun*. 2008;373:151–154.
10. **DeNicola GM, Karreth FA, Humpton TJ, et al.** Oncogene-induced Nrf2 transcription promotes ROS detoxification and tumorigenesis. *Nature*. 2011;475:106–109.
11. **Loignon M, Miao W, Hu L, et al.** Cul3 overexpression depletes Nrf2 in breast cancer and is associated with sensitivity to carcinogens, to oxidative stress, and to chemotherapy. *Mol Cancer Ther*. 2009;8:2432–2440.
12. **Du ZX, Yan Y, Zhang HY, et al.** Proteasome inhibition induces a p38 MAPK pathway-dependent antiapoptotic program via Nrf2 in thyroid cancer cells. *J Clin Endocrinol Metab*. 2011;96:E763–E771.
13. **Zong ZH, Du ZX, Li N, et al.** Implication of Nrf2 and ATF4 in differential induction of CHOP by proteasome inhibition in thyroid cancer cells. *Biochim Biophys Acta*. 2012;1823:1395–1404.

14. **DeLellis RA.** *Pathology and genetics of tumours of endocrine organs*. Lyon, France: IARC Press; 2004.
15. **Papachristou DJ, Sklirou E, Corradi D, Grassani C, Kontogeorgakos V, Rao UN.** Immunohistochemical analysis of the endoribonucleases Drosha, Dicer and Ago2 in smooth muscle tumours of soft tissues. *Histopathology*. 2012;60:E28–E36.
16. **Challeton C, Branea F, Schlumberger M, et al.** Characterization and radiosensitivity at high or low dose rate of four cell lines derived from human thyroid tumors. *Int J Radiat Oncol Biol Phys*. 1997; 37:163–169.
17. **Tanaka J, Ogura T, Sato H, Hatano M.** Establishment and biological characterization of an in vitro human cytomegalovirus latency model. *Virology*. 1987;161:62–72.
18. **Cone RD, Platzer M, Piccinini LA, Jaramillo M, Davies TF.** HLA-DR gene expression in a proliferating human thyroid cell clone (12S). *Endocrinology*. 1988;123:2067–2074.
19. **Ralser M, Querfurth R, Warnatz HJ, Lehrach H, Yaspo ML, Krobitsch S.** An efficient and economic enhancer mix for PCR. *Biochem Biophys Res Commun*. 2006;347:747–751.
20. **Myers MB, McKim KL, Parsons BL.** A subset of papillary thyroid carcinomas contain KRAS mutant subpopulations at levels above normal thyroid [published online ahead of print August 28, 2012]. *Mol Carcinog*. doi:10.1002/mc.21953.
21. **Young O, Crotty T, O'Connell R, O'Sullivan J, Curran AJ.** Levels of oxidative damage and lipid peroxidation in thyroid neoplasia. *Head Neck*. 2010;32:750–756.